

A MODEL FOR COUPLED DYNAMIC ELASTO-PLASTIC ANALYSIS OF SOILS

Mohammred Y. Fattah¹, Saad F. Abbas², and Hussein H. Karim³

ABSTRACT

In this paper a new elasto-plastic material model based on Drucker-Prager plasticity is developed by combining yield and plastic potential functions into a working elasto-plastic model. The dilation slope is derived as a function of the angle of internal friction of the soil and it is considered as a constant parameter of the plasticity model. This assumption is proposed in order to make the material hardening dependent on the angle of friction. This model was implemented into the finite element program OpenSees. A fully coupled dynamic numerical modeling is implemented to predict the dynamic response of saturated soil which is modeled as a two-phase material based on the numerical framework of $u-p$ formulation (u is the displacement of the soil skeleton and p is pore pressure). The first problem represents a homogeneous layer of a saturated natural soil deposit over impermeable bedrock. The dynamic response of this layer showed that the path of the displacement amplitude is varying at each period till reaching to steady state. This behavior is due to irrecoverable (plastic) strain which has occurred in the solid particles of the soil. The second problem studies the dynamic response of an elastic strip footing on saturated soil. It was found that at low viscous coupling (high permeability), the peak of the amplitude of excess pore water pressure decreases at each cycle due to the relatively little dissipation of the water. In contrast, at high viscous coupling (low permeability), the excess pore water pressure builds up to the same peak value, and the amplitude of pore pressure is larger than that at low viscous coupling.

Key words: Coupled, dynamic analysis, model, saturated soil.

1. INTRODUCTION

Soil is not a linear material in which the relations between stress and strain are much more complicated than the simple linearly elastic behavior. Therefore, in order to represent geotechnical problems realistically, some forms of nonlinear relation must be used (Desai and Christian 1977).

The majority of the currently available implementations for predicting coupled soil behavior are based on the $u-p$ formulation. For example, Chan (1988) and Zienkiewicz *et al.* (1999) developed an implementation of the $u-p$ formulation with the generalized theory of plasticity.

In this study, the governing equations for the dynamic fully coupled $u-p$ formulation and appropriate constitutive model are implemented in a developed model which can be used for the practical problems involving saturated soil-foundation systems.

2. DYNAMIC BEHAVIOR OF SOILS

In soil dynamics, concern will be on the response of soils and soil-structure systems to dynamic loads. Common soil dynamics problems include the response of machine foundations to dynamic loads, nondestructive testing of foundation systems and

the response of soil deposits and earth structures to earthquake loads.

Dynamic loadings may produce a wide range of deformations of soils. In the intermediate range, soil deformations vary from small amplitude, nearly elastic, to plastic following earthquakes, water waves, or severe machine-developed forces. Small amplitude deformations of soils are developed adjacent to foundations designed to sustain many stress repetitions without permanent settlements (Richart 1962).

3. TYPES OF NONLINEARITY IN THE ANALYSIS OF POROUS CONTINUA

Two types of nonlinearity exist in the analysis of porous continua, namely, geometric nonlinearity and material nonlinearity.

1. Geometric nonlinearity.

Solid may undergo large or finite deformations; in this case the theory of small deformation is no longer valid (Paul 1982). Therefore, one must resort to the theory of large deformations (Jeremic 2008).

In many applications, for example soft soils, the small deformation assumption is not valid and then the geometric nonlinearity plays a critical role in numerical analysis. Geometric nonlinearity is important when changes in geometry have a significant effect on load deformation behavior. Two examples for geometric nonlinearity are the large movement of slopes and the phenomena of liquefaction (Li and Borja 2005).

2. Material nonlinearity.

In modeling the material nonlinear behavior of solids, plasticity theory is applicable primarily to those bodies that can ex-

Manuscript received March 16, 2012; revised November 25, 2012; accepted December 5, 2012.

¹ Professor (corresponding author), Building and Construction Engineering Dept., University of Technology, Baghdad, Iraq (e-mail: myf_1968@yahoo.com).

² Lecturer, Building and Construction Engineering Dept., University of Technology, Baghdad, Iraq.

³ Professor, Building and Construction Engineering Dept., University of Technology, Baghdad, Iraq.

perience inelastic deformations considerably greater than the elastic deformation. If the resulting total deformation is small enough, then small deformation theory can be applied in solving these problems.

4. COMPUTER PROGRAM

The computer oriented finite element method has become one of the most powerful tools in the analyses of engineering problems. In this paper, the finite element method is used to analyze simple problems in time domain employing the computer program Open System for Earthquake Engineering Simulation (OpenSees). This program was originally produced by University of California.

One of the most flexible, as well as unique, features of OpenSees is the ability to select an analysis procedure that is best for the problem, which is important for tracking structural behavior in the nonlinear range. The solution procedure can be modified during the analysis, allowing for an optimal strategy, depending on convergence criteria. Static and dynamic analysis capabilities are available along with various methods for representing constraints. The analysis procedures are developed to be robust and scalable to large problem sizes. Post-processing is handled in OpenSees by defining recorders of response quantities of interest. OpenSees is a finite element application for which users specify a model and conduct an analysis in OpenSees using a Tool Command Language (TCL) script.

TCL is an interpreted high-level programming language to be easily understandable and easily customizable (Welch *et al.* 2003). The TCL scripting language was chosen to support the OpenSees commands, which are used to define the problem geometry, loading, formulation and solution. These commands are one-line commands which have specific tasks. The TCL language provides useful programming tools, such as variables manipulation, mathematical-expression evaluation and control structures.

TCL is a string-based scripting language which allows the following:

1. Variables and variable substitution
2. Mathematical-expression evaluation
3. Basic control structures (if, while, for, foreach)
4. Procedures

The program is implemented in the C++ programming language through an open-source development process. For a finite element application, to specify a model and conduct analysis the TCL script is used.

The interpreter is an extension of the TCL scripting language. The OpenSees interpreter adds commands to TCL for finite element analysis. Each of these commands is associated with a C++ procedure that is provided. It is this procedure that is called upon by the interpreter to parse the command. For OpenSees the added commands to TCL for finite element analysis are:

1. Modeling: create nodes, elements, loads and constraints
2. Analysis: specify the analysis procedure
3. Output specification: specify what it is monitor during the analysis

OpenSees is an object-oriented framework under construction for finite element analysis. A key feature of OpenSees is the

interchangeability of components and the ability to integrate existing libraries and new components into the framework (Mazzone *et al.* 2007).

The program is comprised of a set of modules to perform creation of the finite element model, specification of an analysis procedure, selection of quantities to be monitored during the analysis, and the output results. In each finite element analysis, an analyst constructs four main types of objects, as shown in Fig. 1.

5. DRUCKER-PRAGER PLASTICITY MODEL FOR SOIL

The Drucker-Prager model is an incremental plasticity theory recognizing the soil as a work hardening material. In this model, the stress at which plastic deformation occurs can be determined from the yield criterion (Owen and Hinton 1980). The function of the yield surface for the model can be expressed by:

$$f = \alpha I_1 + \sqrt{J_2} - \kappa \quad (1)$$

where: I_1 = first stress invariant of the stress tensor, and

J_2 = second invariant of the deviator stress tensor.

The material coefficients α and κ may be not directly obtained from experiments. They are functions of Mohr-Coulomb parameters, the angle of internal friction (ϕ) and cohesion (c) which can be determined by experiments.

$$\alpha = \frac{2 \sin \phi}{\sqrt{3}(3 - \sin \phi)} \quad (2a)$$

$$\kappa = \frac{6 \cos \phi}{\sqrt{3}(3 - \sin \phi)} c \quad (2b)$$

For cohesionless material, $\kappa = 0$, the yield surface becomes:

$$f = \alpha I_1 + \sqrt{J_2} \quad (3)$$

The incremental change in the yield function due to an incremental stress change is (Owen and Hinton 1980):

$$df = \frac{\partial f}{\partial \sigma_{ij}} \quad (4)$$

Then if:

$df < 0$ elastic behavior occurs and the stress point returns inside the yield surface,

$df = 0$ plastic behavior for perfectly plastic material and the stress point remains on the yield surface, and

$df > 0$ plastic behavior for a strain hardening material and the stress point remains on the expanding yield surface.

After initial yielding, the material behavior will be partly elastic. During any increment of stress, the changes of strain are assumed to be divisible into static and plastic components (Yu 2006), so that:

$$d\varepsilon_{ij} = d\varepsilon_{ij}^e + d\varepsilon_{ij}^p \quad (5)$$

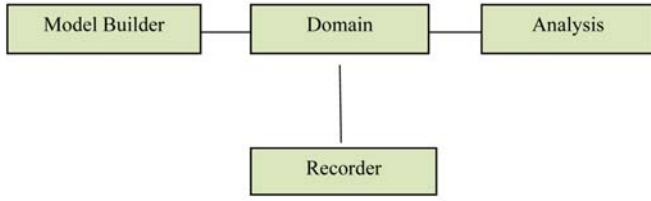


Fig. 1 Main objects in an analysis by the OpenSees program

where $d\varepsilon_{ij}$, $d\varepsilon_{ij}^e$ and $d\varepsilon_{ij}^p$ are the total, elastic and plastic strain increments, respectively.

Before the onset of plastic yielding, the elastic strain increment is related to the stress increment by:

$$d\varepsilon_{ij} = D_{ijkl} d\sigma_{kl} \quad (6)$$

where D_{ijkl} is the tensor of elastic constants for an linear elastic isotropic material, such as soil, has the form:

$$D_{ijkl} = \frac{E}{2(1+\nu)} \left(\frac{2\nu}{1-2\nu} \delta_{ij} \delta_{kl} + \delta_{ik} \delta_{jl} + \delta_{il} \delta_{jk} \right) \quad (7)$$

where: E = modulus of elasticity,

ν = Poisson's ratio, and

δ_{ij} = Kronecker's delta, $\delta_{ij} = 1$ when $i = j$
and $\delta_{ij} = 0$ when $i \neq j$.

At yielding, the incremental plastic strain can be determined from the flow rule which governs the plastic flow after yielding (Yu 2006), so that:

$$d\varepsilon_{ij}^p = d\lambda \frac{\partial Q}{\partial \sigma_{ij}} \quad (8)$$

where $d\lambda$ is a proportionality constant and Q is the plastic potential which is given by:

$$Q = d I_1 + \sqrt{J_2} - \kappa \quad (9)$$

where d = dilation slope.

The Drucker-Prager relations are used as yield criterion in which the associated flow rule implies very large extensional volumetric plastic strains. These are not observed experimentally for soil (Desai and Christian 1977).

The non-associated flow rules used in soils rely on the potential surface which is different from the yield surface. The potential surface must specify the dilation slope as (Jeremic 2008):

$$d = \frac{2 \sin \alpha}{\sqrt{3}(3 - \sin \alpha)} \quad (10)$$

The implementation into OpenSees finite element platform allows use of existing and development of new elasto-plastic material models by simply combining yield functions and plastic potential functions into a working elastio-plastic model. In this study, the dilation slope is derived as a function of the angle of internal friction of the soil and it is considered as a constant parameter of the plasticity model. This assumption is proposed in this work in order to make the material hardening dependent on the angle of friction. To do so, substituting Eq. (2a) in Eq. (10) and rearranging yield:

$$Q = \frac{2}{\sqrt{3}} \left[\frac{\sin \frac{2 \sin \phi}{\sqrt{3}(3 - \sin \phi)}}{3 - \sin \frac{2 \sin \phi}{\sqrt{3}(3 - \sin \phi)}} \right] \quad (11)$$

6. GENERAL FRAMEWORK FOR SIMULATION OF THE SATURATED POROUS MEDIA

There are several different approaches to determine the behavior of a two-phase medium. Generally, they can be classified as uncoupled and coupled analysis. In the uncoupled analysis, the response of saturated soil are computed without considering the effect of soil-water interaction, and then the pore water pressure is calculated separately by means of a pore pressure generation model. In the coupled analysis, all unknowns are computed simultaneously at each time step. These are used for more realistic representation of the physical phenomena than those provided by uncoupled.

In this paper, a fully coupled dynamic numerical modeling is implemented to predict the dynamic response of saturated soil. The saturated soil is modeled as a two-phase material based on the numerical framework of u - p formulation. In this formulation, the displacement of the soil skeleton (u) and pore pressure (p) are the primary unknowns. In addition, this formulation neglects the acceleration of the pore fluid, and neglects the compressibility of the fluid. Using the finite element method for spatial discretization, the u - p formulation is as follows:

$$M \ddot{u} + \int_V B^T \sigma' dV - Q p - f^u = 0 \quad (12)$$

$$H p + Q^T \dot{u} + S \dot{p} - f^p = 0 \quad (13)$$

where:

- M is the mass matrix,
- B is the nodal strain-displacement matrix,
- T is the transpose of a matrix,
- σ' is the effective stress,
- Q is the coupling matrix,
- f is the vector of applied forces,
- H is the permeability matrix, and
- S is the compressibility matrix.

The effective stress σ' can be determined by the soil constitutive model. To complete the numerical solution, it is necessary to integrate the above equations in time. Here, the original Newmark method is used.

The generalized Newmark method can be considered as a generalization of Newmark's two parameter time integration scheme. In all time stepping schemes, the value x_n can either be the displacement or the pore water pressure and its derivatives \dot{X}_n and \ddot{X}_n at time t_n with the values of X_{n+1} , \dot{X}_{n+1} and \ddot{X}_{n+1} which are valid at time t_{n+1} and are the unknowns.

7. SOIL-PORE FLUID INTERACTION

Frequently two or more physical systems interact with each other, with the independent solution of any system being impos-

sible without simultaneous solution of the others, such systems are known coupled. The behavior of soils is strongly influenced by the pressures of the fluid present in the pores of the material (Zienkiewicz and Taylor 2005).

Pore fluid-solid interaction is important in material like saturated soil under dynamic conditions. This material when saturated with fluid can be treated as two-phase material, *i.e.* the solid skeleton and the fluid in the voids (Paul 1982).

8. LINEAR ELASTIC DYNAMIC RESPONSE OF ONE-DIMENSIONAL SOIL COLUMN

To show the validation of the *u-p* formulation, the dynamic behavior of a finite saturated half space that is subjected to sinusoidal loading function of the form $F(t) = F_o \sin(\omega t)$ is studied.

The problem represents a homogeneous layer of a saturated natural soil deposit over impermeable bedrock. For the finite element discretization, an elastic soil column is considered to represent the saturated soil. This model is implemented for the three-dimensional description of the stress-strain response of the soil. Therefore, an element of 8-node hexahedral linear isoparametric is used to model the soil column as shown in Fig. 2. Each element node has four degrees of freedom; the first, second and third degrees of freedom are for solid displacements (*u*) while the fourth degree of freedom is for fluid pressure (*p*).

To achieve a one-dimensional analysis, the boundary conditions are applied so that the bottom of the soil column is fixed in solid displacement while the top surface of the soil is set to be free in solid displacement (pore pressure $p = 0$). All the intermediate nodes are fixed in *x-y* plane, but the vertical movement is allowed.

A time step ($\Delta t = 0.1$ sec) is used in the Newmark method to integrate the aforementioned Eqs. (12) and (13) in time. A uniform vertical pressure of ± 100 kPa is applied on the top surface of the soil column, with loading period of 100 seconds. The boundary conditions are applied in a manner that the bottom of the soil column is fixed in solid displacement while the top surface of the soil is set to be free in solid displacement and therefore the pore water pressures at the free surface are taken as zero (Paul 1982).

The material parameters for the half space elastic response are shown in Table 1. To cure the artificial oscillation, the numerical damping is introduced into the analysis by using $\gamma = 0.6$ and $\beta = 0.3025$ in the Newmark algorithm (Jeremic 2006). The results of the solution from the present study are shown in Figs. 3, 4 and 5. It can be noted that when the solid part moves upward (see Figs. 4 and 5), the pore water pressure displays negative values (pore fluid suction) as shown in Fig. 5.

The larger displacement of the solid skeleton occurs when it is closer to the surface. This phenomenon can be explained by considering elastic recovery of the solid skeleton.

Jeremic (2006) gave the numerical solution of this problem by the *u-p-U* formulation as shown in Fig. 6 to simulate the solid skeleton and pore water pressure responses. This formulation allows, among other features, for fluid acceleration to be taken into account. The symbol “*U*” refers to the relative displacement of water (fluid) with respect to soil solids. By comparing the results of the present study with those given by Jeremic (2006), good agreement is shown. The differences in solid displacement

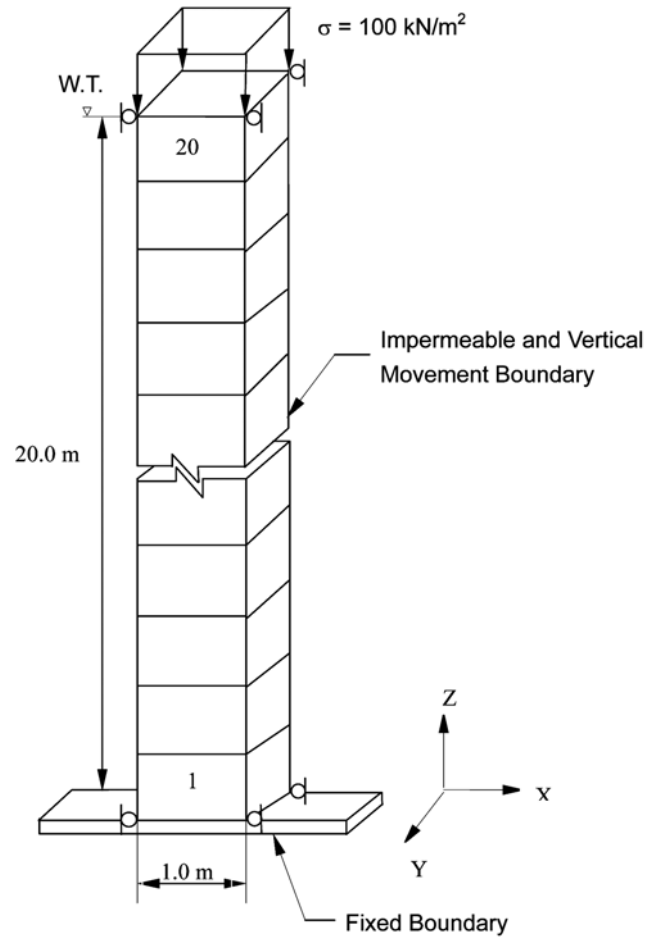


Fig. 2 Finite element idealization of the soil deposits subjected to vertical harmonic vibration

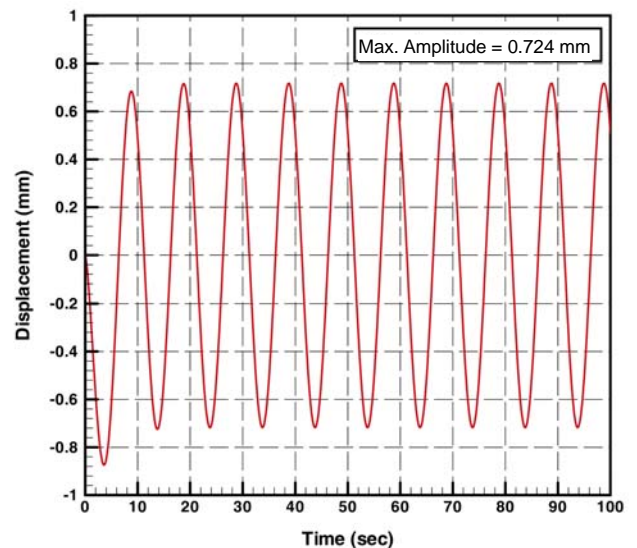


Fig. 3 The predicted elastic response of solid particles, displacement - time history at surface

and pore water pressure can be attributed to the inclusion of dilation as a function of the angle of internal friction of the soil and considered as a constant parameter of the plasticity model.

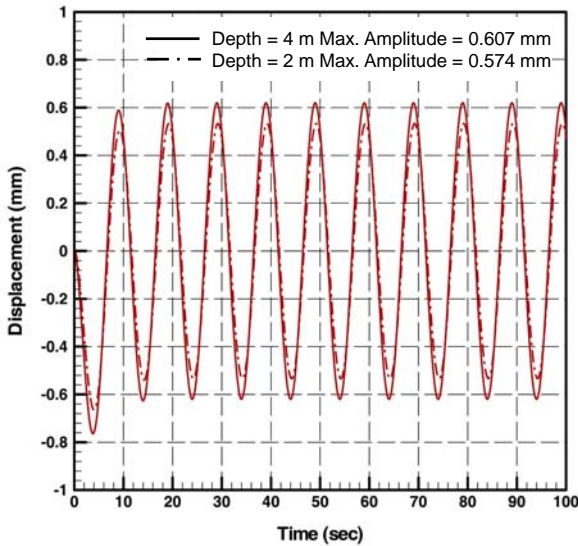


Fig. 4 The predicted elastic response of solid particles, displacement-time history at 2 m and 4 m depth

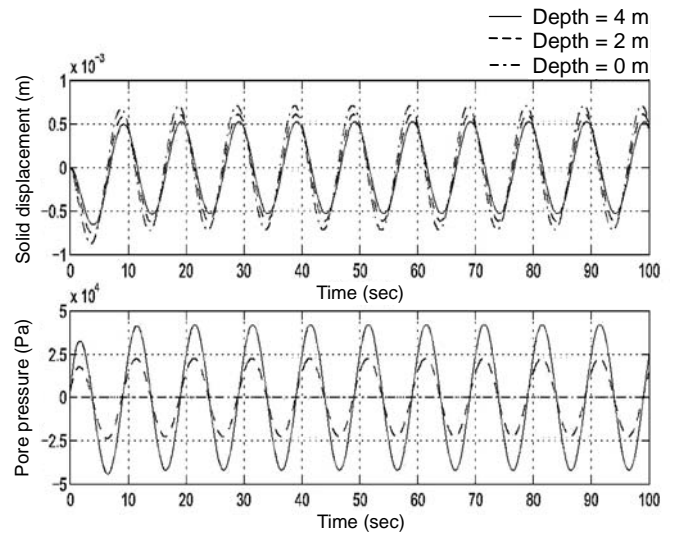


Fig. 6 The elastic response of solid particle displacement and pore pressure with time histories (after Jeremic 2006)

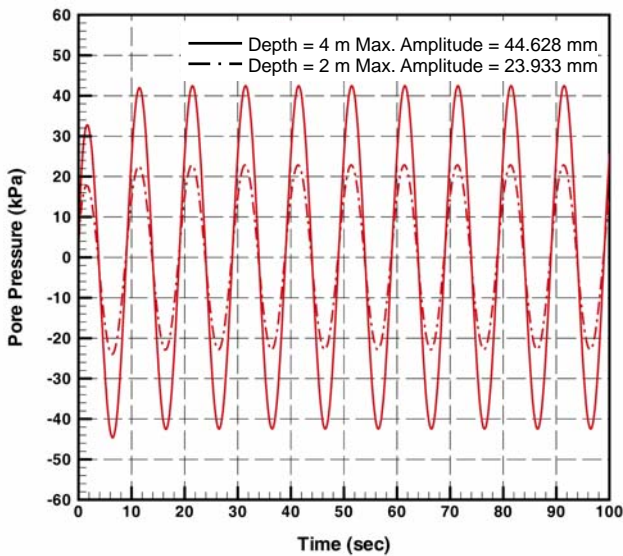


Fig. 5 The predicted elastic response of pore water pressure-time history at 2 m and 4 m depth

Table 1 Material parameters of the soil for elastic response (from Jeremic 2006)

Parameters		Value
Poisson's ratio	ν	0.20
Modulus of elasticity (kN/m ²)	E	1.2×10^6
Mass density of soil (kg/m ³)	ρ	2.0×10^3
Mass density of fluid (kg/m ³)	ρ_f	1.0×10^3
Bulk modulus of fluid (kN/m ²)	K_f	1.0×10^{20}
Coefficient of permeability (m/sec)	k	3.6×10^{-4}

9. ELASTO-PLASTIC DYNAMIC RESPONSE OF ONE-DIMENSIONAL MODEL

As noticed above, deformation may be classed as recoverable or unrecoverable. The saturated soil column as shown in Fig. 2 is reanalyzed for the same dynamic load and time step. The solid skeleton of the soil is represented by the Drucker-Prager plasticity model with non-associative flow rule as developed in this paper. The elastic properties of the soil are shown in Table 1. Accordingly, the recommended angle of internal friction is 35° and thus $\alpha = 0.273$ and $d = 1.84 \times 10^{-3}$.

The dynamic response of the soil column is shown in Figs. 7, 8 and 9. It can be shown that the path of the amplitude of the displacement is varying at each period till reaching a steady state (Figs. 7 and 8). This behavior is due to irrecoverable (plastic) strain which has occurred in the solid particles of the soil. In addition, the fluid phase response is linear elastic (Fig. 9); this verifies that the plastic behavior is essentially independent of hydrostatic pressure (Owen and Hinton 1980).

This study indicates that the dynamic response of the solid displacement and pore pressure from the elasto-plastic behavior is larger than that assuming elastic behavior of the soil.

10. TWO-DIMENSIONAL DYNAMIC ANALYSIS OF FOUNDATIONS ON SATURATED SOIL

In this section, the proposed numerical model is implemented for the analysis of soil-structure interaction. The soil is modeled as an elasto-plastic solid where the Drucker-Prager plasticity model with a non-associative flow rule is adopted to include the effects of the soil nonlinearity. Due to the fact that the analysis of very large models take too long time to run on a single computer processor, a two-dimensional quasi-plane-strain is proposed as a simplification to the full three-dimensional model.

To study the dynamic response of an elastic strip footing, a soil-foundation system has to be considered. The geometry of the problem consists of a concrete strip footing of width $B = 2$ m and thickness of 0.25 m resting on a saturated sand. The soil-foundation system is subjected to a sinusoidal loading applied on

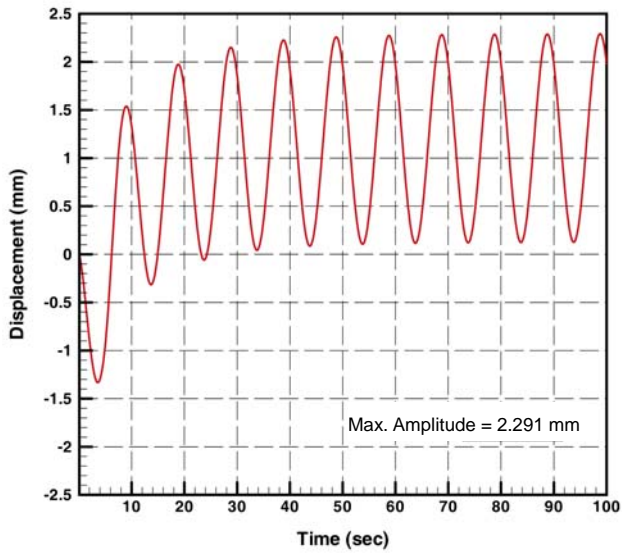


Fig. 7 The predicted elasto-plastic response of solid partials displacement with time histories

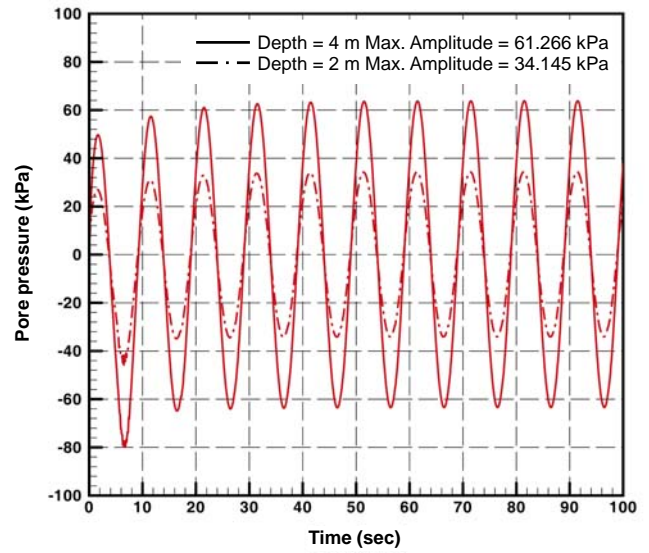


Fig. 9 The predicted elasto-plastic response of pore pressure time histories at 2 m and 4 m depth

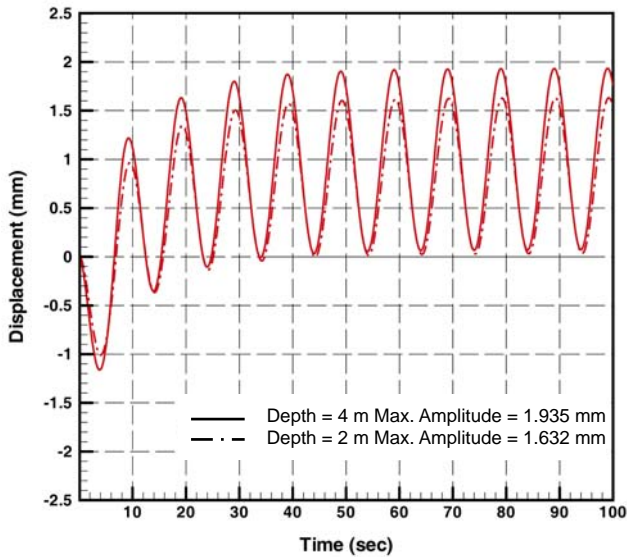


Fig. 8 The predicted elasto-plastic response of solid partials displacement time histories at 2 m and 4 m depth

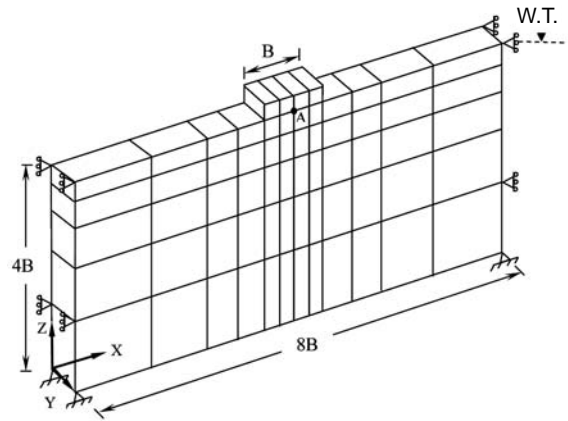


Fig. 10 Two-dimensional quasi-plane-strain model

the top surface of the footing. The amplitude of the pressure is ± 10.0 kPa and the period of the loading is 10 sec. The soil medium is discretized using brick elements which have eight nodes for the solid phase, with three degrees of freedom in the x , y and z direction at each node, and eight nodes for the fluid phase as shown in Fig. 10.

The soil properties are considered to be uniform throughout the depth of the layer which is a common assumption in soil dynamics, the material properties of the saturated sand are shown in Table 2. Assuming that the modulus of elasticity of the soil E_s is constant and the material stiffness of the foundation E_f maintains the ratio of E_s / E_f which is 1/100. The above sentence refers to the initial values of the modulus of elasticity of the soil E_s which will be changed with stress level during the analysis. The bulk density and Poisson's ratio for the material of the footing are 2.4 ton/m^3 and 0.20, respectively.

Table 2 Material parameters of the saturated sand (after Chan and Ou 2008)

Parameters		Value
Poisson's ratio	ν	0.31
Modulus of elasticity (kPa)	E	1.95×10^5
Mass density of soil particles (kg/m^3)	ρ_s	2670
Bulk modulus of soil particles (kN/m^2)	K_s	1.0×10^{17}
Mass density of fluid (kg/m^3)	ρ_f	1000
Bulk modulus of fluid (kN/m^2)	K_f	1.0×10^6
Porosity	n	0.398
Angle of internal friction (degree)	ϕ	35

The boundary conditions are applied so that the nodes lying in a plane parallel to the Y - Z plane at $X = 0.0$ m and 16.0 m are restrained in X -direction. For nodes lying in the planes parallel to the X - Z plane are restrained in Y -direction. A fully restrain is considered for all nodes in X - Y plane at $Z = 0.0$ m.

Two different coefficients of permeability (*i.e.* $k = 1 \times 10^{-3}$ and $k = 1 \times 10^{-5}$ m/sec) are selected to show the effects of viscous coupling between the solid and fluid parts. The responses of the foundation due to sinusoidal loading at different permeability are presented in Figs. 11, 12, 13 and 14.

From Figs. 11 and 13 it can be found that the permanent deformation in the soil occurs due to the plastic strain in the solid skeleton. Figures 12 and 14 show that at low viscous coupling ($k = 1 \times 10^{-3}$ m/sec), the peak of the amplitude of excess pore water pressure decreases at each cycle due to the relatively little dissipation of the water. In contrast, at high viscous coupling ($k = 1 \times 10^{-5}$ m/sec), the excess pore water pressure builds up to the same peak value, and the amplitude of pore pressure is larger than that at low viscous coupling ($k = 1 \times 10^{-3}$ m/sec).

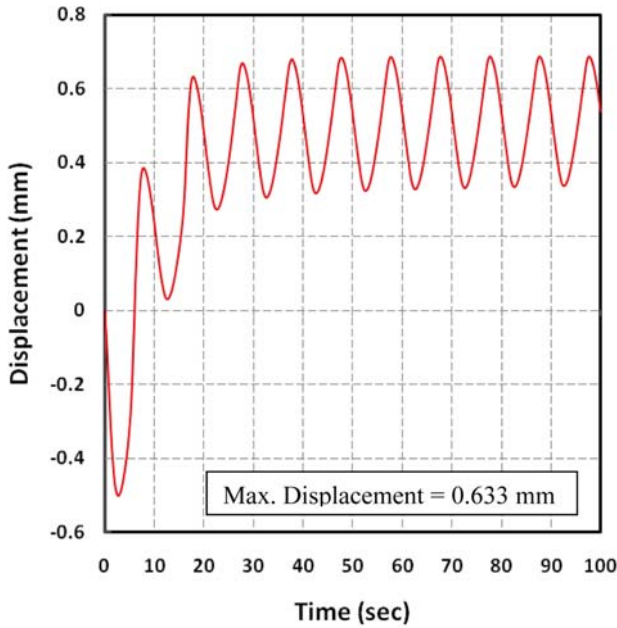


Fig. 11 Displacement response of the strip footing at point A ($k = 1 \times 10^{-3}$ m/sec)

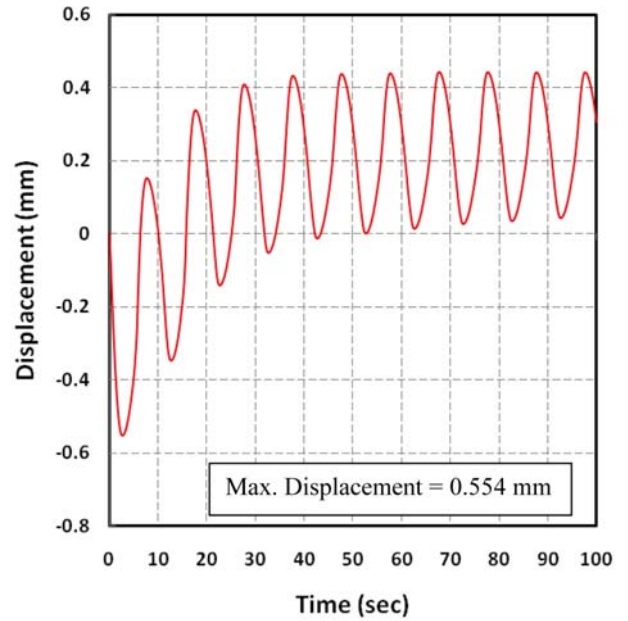


Fig. 13 Displacement response of the strip footing at point A ($k = 1 \times 10^{-5}$ m/sec)

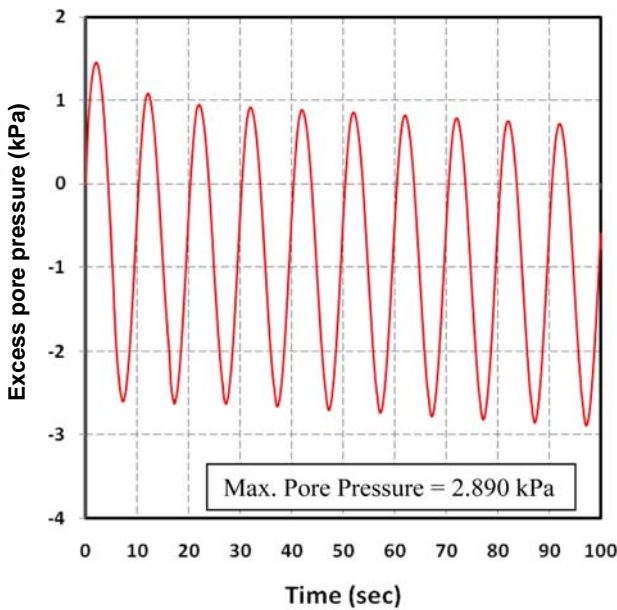


Fig. 12 Excess pore water pressure under the strip footing at point A ($k = 1 \times 10^{-3}$ m/sec)

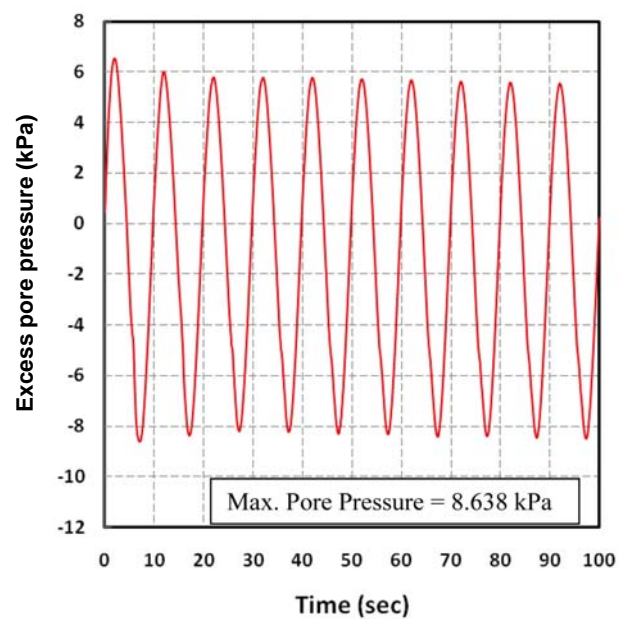


Fig. 14 Excess pore water pressure under the strip footing at point A ($k = 1 \times 10^{-5}$ m/sec)

11. CONCLUSIONS

1. In this work, a new elasto-plastic material model based on Drucker-Prager plasticity is developed by simply combining yield functions and plastic potential functions into a working elasto-plastic model. The dilation slope is derived as a function of the angle of internal friction of the soil and it is considered as a constant parameter of the plasticity model. This assumption is proposed in order to make the material hardening dependent on the angle of friction. In this work a new elasto-plastic material model based on Drucker-Prager plasticity is developed by simply combining yield and plastic potential functions into a working elasto-plastic model.
2. The dynamic response of a homogeneous layer of a saturated natural soil deposit over impermeable bedrock showed that the path of the displacement amplitude is varying at each period till reaching to steady state. In addition, the fluid phase response is linear elastic. The dynamic response of the solid displacement and pore pressure from the elasto-plastic behavior is larger than that assuming elastic behavior of the soil.
3. At low viscous coupling, the peak of the amplitude of excess pore water pressure decreases at each cycle due to the relatively little dissipation of the water. In contrast, at high viscous coupling, the excess pore water pressure builds up to the same peak value, and the amplitude of pore pressure is larger than that at low viscous coupling.

REFERENCES

- Chan, A. H. C. (1988). "A unified finite element solution to static and dynamic geomechanics problems." Ph.D. Thesis, University College of Swansea, UK.
- Chan, A. H. C. and Ou, J. (2008). "Three-dimensional numerical analysis of a dynamic structure, saturated soil and pore fluid interaction problem." in M. Papadarakakis, B.H.V. Topping, Eds., *Trends in Engineering Computational Technology*, Saxe-Coburg Publications, Stirlingshire, UK, Chapter 17, pp. 335–353.
- Desai, C. S. and Christian, J. T. (1977). *Numerical Methods in Geotechnical Engineering*, McGraw-Hill Book Co., Inc., London.
- Jeremic, B. (2006). "Computational geomechanics: Inelastic finite elements for pressure sensitive materials." Lecture Note, University of California, Davis, USA.
- Jeremic, B. (2008). "Computational geomechanics: Inelastic finite elements for pressure sensitive materials." Lecture Note, University of California, Davis, USA.
- Li, C. and Borja, R. I. (2005). "Finite element formulation of poroelasticity suitable for large deformation dynamic analysis." Report No. 147, Department of Civil and Environmental Engineering, Stanford University, USA.
- Mazzoni, S., McKenna, F., Scott, M., and Fenves, G. (2007). "Open-sees command language manual." *Pacific Earthquake Engineering Center*, University of California, Berkeley, USA.
- Owen, D. R. and Hinton, E. (1980). *Finite Elements in Plasticity: Theory and Practice*, Pineridge Press, Swansea, UK.
- Paul, D. K. (1982). "Efficient dynamic solutions for single and coupled multiple problems." Ph.D. Thesis, University College of Swansea, UK.
- Richart, F. E. (1962). "Foundation vibrations." *Journal of Soil Mechanics and Foundations Division*, ASCE, **127** (Part I), pp. 207–220.
- Yu, H. S. (2006). "Plasticity and geotechnics." *Advances in Mechanics and Mathematics Series*, **13**, Springer Science and Business Media, LLC.
- Welch, B., Jones, K., and Hobbs, J. (2003). *Practical Programming in TCL and TK*. Fourth Edition, Pearson Education Ltd.
- Zienkiewicz, O. C., Chan, A., Pastor, M., Schrefler, B., and Shiomi, T. (1999). *Computational Geomechanics with Special Reference to Earthquake Engineering*, John Wiley and Sons Ltd., England.
- Zienkiewicz, O. C. and Taylor, R. L. (2005). *The Finite Element Method for Solid and Structural Mechanics*, Sixth Ed., Elsevier Butterworth-Heinemann, UK.